http://dx.doi.org/10.21577/0100-4042.20170883 *Quim. Nova,* Vol. 45, No. 6, 674-679, 2022

Artigo

QUANTITATIVE SPECIATION OF THE LIQUID PHASE BY FTIR SPECTROSCOPY IN THE SYSTEM AMP-PZ-CO_2-H_2O

Armando Zanone[a,b,*], Denise T. Tavares[b] e José L. de Paiva[b]
[a]Departamento de Engenharia Química, Instituto Mauá de Tecnologia, 09580-900 São Caetano do Sul – SP, Brasil
[b]Departamento de Engenharia Química, Escola Politécnica da Universidade de São Paulo, 05508010 São Paulo – SP, Brasil

Recebido em 02/09/2021; aceito em 13/01/2022; publicado na web em 24/03/2022

This work reports a multivariate calibration partial least square regression (PLS) model to quantify the liquid-phase concentrations of 2-amino-2-methyl-1-propanol (AMP), piperazine (PZ), bicarbonate, PZ monocarbamate, and PZ dicarbamate during the absorption/desorption process by Fourier Transform Mid-Infrared spectroscopy (mid-FTIR). The model could predict 33 different concentrations ranging from 0 to 40 wt.% AMP, 0 to 15 wt.% PZ, and 0 to 12 wt.% total CO_2 with relative errors lower than 10%, and 87% of the variance of all samples have been represented (R^2), except for PZ dicarbamate. A comparison of a single PLS2 model was made with multiple PLS1 models, one for each chemical species present in the liquid phase. The latter had better predictions and made it possible to differentiate CO_2 from its chemical forms, allowing a better understanding of the CO_2 capture processes.

Keywords: amine blend; carbamate; carbon capture; infrared spectroscopy.

INTRODUCTION

The CO_2 capture process is one important and challenging issue of the moment, motivating intense research and investments.[1-5] The principal technology used to reduce CO_2 emissions is the chemical absorption process using aqueous amine solutions[6] due to its higher removal rate and efficiency in dilute gas streams.[1-3] The main drawback of this process is the high energy required to regenerate the solvent.[7,8]

The use of the 2-amino-2-methyl-1-propanol (AMP) and piperazine (PZ) mixture as a solvent has the advantage of AMP requiring a low energy demand for its regeneration, despite the moderate rate of absorption with CO_2. And PZ provides higher reaction velocity at the expense of average energy demand for desorption.[2,8] This mixture of solvents was extensively studied, highlighting its advantages.[4,5,9-12]

The determination of an accurate mass transport coefficient is necessary to design, optimize and evaluate different capture processes.[13] Thus, it is required to know the composition of the chemical components present in both phases to characterize the process. Fourier transform infrared (FTIR) spectroscopy integrated with the multivariate regression method allows the simultaneous quantification of the chemical species in a fast, non-invasive manner, and ensures the integrity of the samples, ideal characteristics for online monitoring of the CO_2 capture process.[14,15]

FTIR has been used to study CO_2 capture processes. Mergler *et al.*[16] identified the spectrum bands associated with reaction products of the MEA-CO_2-H_2O system. Geers *et al.*[17] built a PLS model to estimate the CO_2, SO_X, and β-alanine concentration from FTIR spectra in a post-combustion capture pilot plant. Diab *et al.*[13] used FTIR spectroscopy to speciate the liquid phase in an aqueous solution of diethanolamine (DEA) and CO_2 systems for different CO_2 loadings, mass fractions, and temperatures. van Eckeveld *et al.*[18] developed inverse least-squares models for the online liquid analysis of the MEA-CO_2-H_2O system using FTIR spectroscopy, density, conductivity, refractive index, and sonic speed measurements as input data. van der Ham[19] included solvent degradation products of an MEA-CO_2-H_2O system in the calibration model and obtained worse predictions. Kachko *et al.*[15] built a model to quantify MDEA, PZ, and CO_2 concentration based on the NIR spectra, density, pH, conductivity, sound velocity, and refractive index. Kachko *et al.*[20] compared the prediction of captured CO_2 concentration in aqueous MEA solutions using Raman, NIR, and ATR-FTIR spectroscopy. du Preez *et al.*[21] developed an FTIR spectroscopy method to study the CO_2 reaction with monoethanolamine (MEA) in an n propanol solvent. They collected real-time reaction kinetic data using an attenuated total reflectance (ATR) probe confirming that the zwitterion reaction mechanism accurately describes the MEA reaction in a non-aqueous system.

FTIR was used to identify the amines, carbamates, and bicarbonate during the CO_2 absorption in aqueous solutions of AMP.[22,23] And for cyclic amines (e.g., PZ).[24] Ermatchkov *et al.*[25] used 1HNMR spectroscopy to speciate an aqueous PZ-CO_2 system. Kachko *et al.*[14] monitored an absorption process using an AMP-PZ solvent. They used NIR spectroscopy and physical data to build a chemometric model. However, they did not work with CO_2-saturated amines. Li *et al.*[26] developed a rigorous thermodynamic model in Aspen Plus using the electrolyte non-random two liquid activity coefficient (e-NRTL) model for the system PZ-AMP-CO_2-H_2O and compared to NMR speciation. Zanone *et al.*[9] simultaneously quantified AMP, PZ, and total CO_2 in all its chemical forms in the liquid phase. However, they did not distinguish carbamates, carbonates, or soluble CO_2.

The main drawback of the absorption using aqueous solutions of amines to absorb CO_2 is the high energy needed to regenerate the solvent.[8,27] This energy is directly related to the stability of the chemical products formed during the reaction with the amines. Carbamates formed due to reaction with primary amines (e.g., MEA) are more stable than carbamates formed from secondary amines (e.g., DEA), for example. Consequently, less energy is required to regenerate the latter.[28] Furthermore, this means that knowing the CO_2 concentration in these solvents is not enough, as the different chemical forms of CO_2 will have an impact on the energy needed and the desorption rates.

This study aimed to develop an FTIR spectroscopy method for online speciation of the liquid phase of the chemical absorption/desorption process of the AMP-PZ blend solvent over the entire

*e-mail: armando.zanone@maua.br

Table 1. Concentration of the non-carbonated samples

Sample	1	2	3	4	5	6	7	8	9	10	11	12	13
AMP (wt.%)	5	10	15	20	25	30	35	40	0	0	0	0	0
PZ (wt.%)	0	0	0	0	0	0	0	0	3	6	9	12	15
Sample	14	15	16	17	18	19	20	21	22	23	24	25	26
AMP (wt.%)	28	26	24	22	20	18	15	30	0	0	21	12	5
PZ (wt.%)	2	4	6	8	10	12	0	0	4.5	9	9	3	15

range of CO_2 loadings. We used PLS models to differentiate the CO_2 in its different chemical forms (i.e., carbamates and carbonates). Furthermore, we compare the amines quantification using a PLS and a PLS2 model.

MATERIALS AND METHOD

Samples

All the calibration curves standard samples were prepared gravimetrically on an analytical scale model AY220, Shimadzu. AMP (Sigma Aldrich), PZ (Sigma Aldrich), distilled water, and CO_2 (99.9%, Air Liquide Brasil) were the reagents used. The non-carbonated samples were: eight aqueous AMP solutions ranging from 5 to 40 wt.%; five aqueous PZ solutions from 3 to 15 wt.%; and six AMP-PZ blends, as shown in Table 1.

Since there is no analytical standard for AMP and PZ carbamates, we prepared these samples as already reported in our past work.[9] These standard samples consisted of the samples 20 to 26 from Table 1 prepared gravimetrically. Each aqueous amine solution was constantly stirred and bubbled with an equal volume rate of air and CO_2 at atmospheric pressure, as shown in Figure 1.

Every 30 s, the bubbling was paused, and one spectrum of the sample was collected, then the bubbling was resumed. The total bubbling time was determined by the infrared (IR) spectrum, stopping the reaction (bubbling) when the IR spectra did not change, indicating that the chemical equilibrium had been established. The ending of the reaction could also be determined by the temperature of the solution that stops increasing. The reference concentration of AMP, PZ, and total CO_2 in the liquid phase was obtained by potentiometric titration using 0.5 mol L^{-1} HCl.

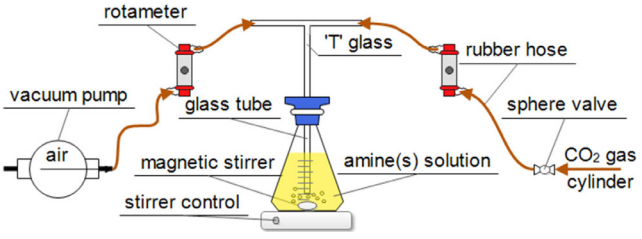

Figure 1. *Carbonation process of the standard samples*

MIR spectra acquisition

The spectra were collected using the ReactIR 45m Fourier Transform Infrared (FTIR) spectrometer from Mettler-Toledo with a diamond sensor microflow cell and Mercuric-Cadmium-Telluride detector (MCT). A dedicated computer running the software iC IR™ v4.2.26 controlled the FTIR. The measured frequency was in the range of 650-4000 cm^{-1} at a spectral resolution of 4 cm^{-1} with 32 scans. The liquid probe temperature was maintained at 303 K by a controller. The software subtracted the water spectrum from all samples as a background. For each solution, up to 20 spectrum samples were collected. As CO_2 bubbles could form during the spectrum acquisition, we discarded these anomalous spectra.

Liquid speciation

We used potentiometric titration (TitroLine easy, Schott Instruments) using 0.5 M HCl to obtain the concentration of AMP and PZ from samples 1 to 13 (non-carbonated pure amines standard samples) in triplicate. Since the equivalence points of AMP and PZ overlap, we calculated the concentration reference value based on the gravimetric data corrected by the purity of the individual amines according to the previous analysis procedure.[9,29,30] After the carbonation, the titration resulted in the total CO_2 absorbed in all its chemical forms.[9,29,30]

The titration method could not distinguish among the different CO_2 species (i.e., bicarbonate, PZ mono- and dicarbamate). And there was no access to other analytical equipment to overcome this problem (e.g., NMR spectroscopy). AMP reacts with CO_2 to form AMP carbamate and rapidly reacts with another base resulting in bicarbonate and protonated AMP.[3,9,23,31] Additionally, the carbamate formation is ten times lower than the bicarbonate.[31] Therefore, we considered that all CO_2 quantified in the saturated solutions of AMP was bicarbonate.

Furthermore, PZ reacts with CO_2 to form PZ monocarbamate ($PZCOO^-$), which could react again with CO_2 to form PZ dicarbamate ($^-OOCPZCOO^-$).[9,23,24] Consequently, all CO_2 quantified in the saturated solutions of PZ was considered as only PZ dicarbamate. And, we considered that the first spectrum acquired (first 30 seconds of CO_2 absorption) referred to PZ monocarbamate only.

Models

We generated multiple PLS models, one model for each chemical species: non-reacted AMP, nonreacted PZ, bicarbonate, PZ monocarbamate, and PZ dicarbamate. The region used was obtained as reported in past work[9] using a changeable size moving window (CSMW)[32] using a script written in MATLAB. The same region was implemented in the models built in the equipment software iC IR™ v4.2.26 to validate the MATLAB script and allow online quantification of the samples.

Altogether, 568 spectra samples were used divided into 270 spectra training-set and 298 spectra validation-set using a leave-one-out cross-validation. It was used 20 spectra for all 26 solutions described in Table 1 randomly separated into the training and validation sets, and 10 spectra for the 7 carbonated solutions prepared from the reaction of samples 20 to 26 (Table 1) with CO_2. From the solutions with CO_2, only the saturated sample spectra were randomly chosen to be in the training set, while the partially carbonated solution was all present in the validation set.

All data were mean-centered, and other pretreatments were made specifically for each species, as detailed in Table 4. Also, the wavenumber range used in the PLS model was different for each species. The minimum root-mean-square error of prediction (RMSEV) determined the number of factors.

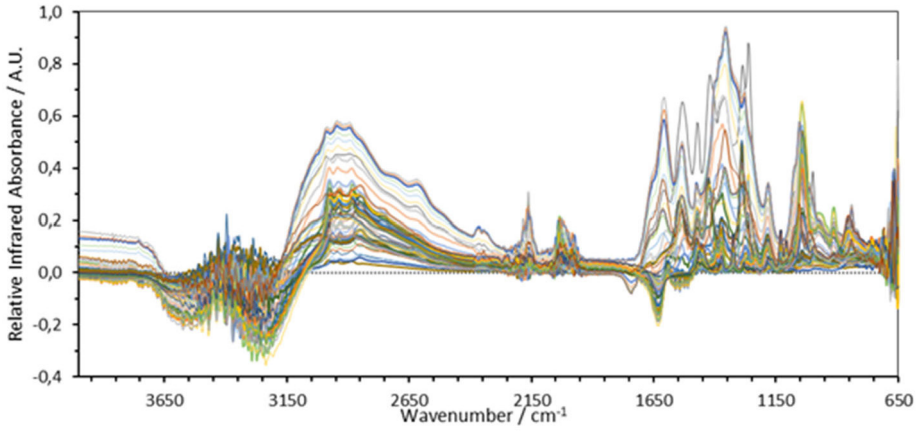

Figure 2. *MIR spectra for all amines concentrations samples with subtracted water spectrum*

Table 2. IR peaks assignments for carbonated AMP and PZ solutions

Wavenumber (cm^{-1})	Band attribution	Specie concerned	References
1636	δasNH3+	AMPH+	9, 23
1534	δsNH3+	AMPH+	9, 23
1382	νasC-O	HCO3-	9, 23, 24
1355	νsC-O	HCO3-	9, 23, 24
1072	νC-N	AMPCOO-, AMPH+	9,23
1054	νC-O	AMPCOO-, AMPH+	9,23
1044	νC-N and νC-O overlap	AMP	9,23
915	τN-H	AMP	9,23
840	γCO_3	HCOO-	33,34
1546, 1524	$vasCOO^-$	PZCOO- -OOCPZCOO-	9,24
1470	δsNH2+	PZH+ and +HPZH+	9,24
1289 1265	vasN-COO^- and vsN-COO^- overlap	PZCOO- -OOCPZCOO-	9,24
1087, 1130, 1100	νmCN	PZ	

RESULTS AND DISCUSSION

Figure 2 shows the spectra of all 33 different concentrations solutions (26 concentrations shown in Table 1 plus 7 carbonated solutions) used to build the PLS models.

Spectra information

Table 2 summarizes the wavenumber, the band attribution, and the species concerned. We used these as the starting window for the CMSW method to build the PLS models. Table 4 specifies the final region chosen.

Samples

The titration in triplicate of all samples is on the supplementary material. Comparing the weighed mass and the titration concentration allowed us to predict the AMP and PZ purities as 91±1% and 98±1%, respectively. The titration standard deviation error was 0.08 wt.%.

PLS2 model

We already developed a single PLS2 model to predict AMP, PZ, and CO_2 absorbed in all its chemical forms (i.e., carbamates and carbonates).[9] This model was obtained with a single-window at 1690-846 cm^{-1} without any pretreatment using 8 factors.[10] Altogether, 568 spectra samples had their concentration predicted with relative errors lower than 10% and 93% of the variance of the samples represented. Although the data variance could be well reproduced ($R^2 > 0.999$ and $Q^2 > 0.9$), as shown in Table 3, it had a drawback in predicting the PZ concentration in some of the CO_2 saturated solutions. This probably happens due to the PZ peak at 1326 cm^{-1} that gets overlapped by the PZ carbamates formation.[9] Table 3 shows the training coefficient of determination (R^2), the validation coefficient of determination (Q^2), the root-mean-square error of calibration (RMSEC), and the root-mean-square error of prediction (RMSEP).

Table 3. Coefficient of determination and root-mean-square errors for the PLS2 model

Component	Factors	R^2	Q^2	RMSEC	RMSEP
AMP		0.99999	0.93252	0.1530	0.825
PZ	9	0.99988	0.98172	0.1400	0.904
CO_2		0.99999	0.99398	0.0186	0.223

PLS models

We developed one PLS model for each chemical component identified in the liquid phase: AMP, PZ, HCO_3^-, $PZCOO^-$, and $^-OOCPZCOO^-$.[9] The models' specifications are shown in Table 4.

Table 4. PLS specifications for each species model

Species concerned	Region (cm^{-1})	Pre-Treatment	Factors
AMP	1082-1026	9 points Savitz-Golay	10
PZ	1140-1080	9 points Savitz-Golay	7
$PZCOO^-$	1303-1250	second derivative	1
$^-OOCPZCOO^-$	1303-1250	none	1
HCO_3^-	845-836	second derivative	1

The region in 1303-836 cm^{-1} contained all the information used in all models, meaning we could gather more information with less data than the PLS2 model. Figure 3 shows the regions used in the model.

The AMP model used the C-N stretching band (ν) region, which decreased and shifted, distinguishing from the νC-O as AMP got protonated to $AMPH^+$. The PZ was predicted based on the disappearance of the medium stretching (νm) of the CN band. The PZ carbamates models ($PZCOO^-$ and $^-OOCPZCOO^-$) used the symmetrical and asymmetrical νN-COO^- bands. As both overlaps, we applied a second derivative pretreatment to distinguish them. Finally, the bicarbonate model used the out-of-plane deformation γCO_3 mode.

Altogether, 568 spectra samples had their concentration predicted with relative errors lower than 10% and 87% of the variance of all samples represented. Table 5 shows the R^2, Q^2, RMSEC, and RMSEP. The model drawback is the PZ dicarbamate with half R^2 compared to the other species. Probably, the assumption that the CO_2 saturated PZ solutions contained only PZ dicarbamate is weak. Probably dicarbamate converted to bicarbonate at rich loadings.[26]

Figure 4 (a) compares the concentration predicted by the PLS model and the titration reference value. The residues are shown in Figure 4 (b) and seem random. Since the titration does not distinguish the CO_2 absorbed into its different chemical forms, we only present in Figure 4 the amines and total CO_2 concentration.

Figure 5 shows the prediction of the mono- and dicarbamate of PZ and bicarbonate in the 5 wt.% AMP 15 wt.% PZ blend during the carbonation process. At the beginning of the reaction, there was a rapid formation of $PZCOO^-$ which then reaches a maximum concentration. At the same time, monocarbamate is transforming into $^-OOCPZCOO^-$ at a lower rate and rapidly after the monocarbamate reaches the maximum concentration. This faster dicarbamate formation is associated with the total consumption of free PZ. Although the $^-OOCPZCOO^-$ prediction is not reliable, this profile agreed with published works.[9,23,24]

In the blend, AMP acts as a base that catalyzes the PZ reaction with CO_2, then HCO_3^- does not have a significant concentration. Moreover, a higher spectral noise present at wavenumbers below 900 cm^{-1} reflect a higher deviation on the bicarbonate concentration prediction.

Models comparisons

In this section, we compare our newly developed PLS models

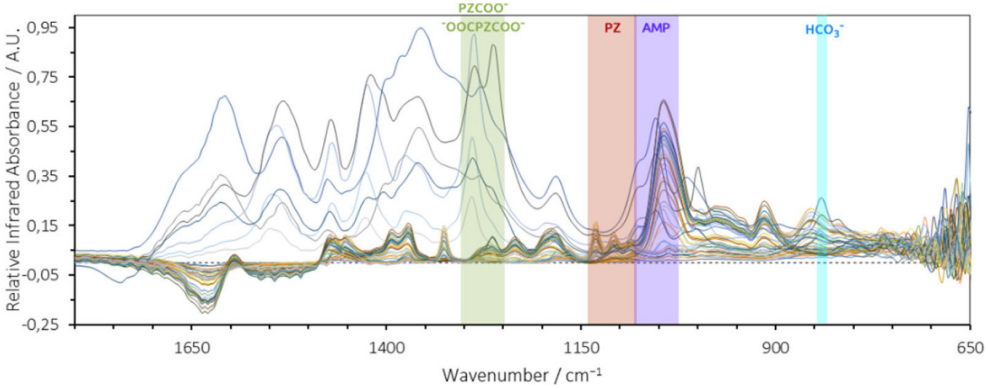

Figure 3. *MIR spectra for all samples highlighted the regions used*

Table 5. Coefficient of determination and root-mean-square errors for the PLS models

Component	Factors	R^2	Q^2	RMSEC	RMSEP
AMP	10	0.99999	0.99733	0.1268	1.5400
PZ	7	0.99999	0.99398	0.1804	0.6517
$PZCOO^-$	1	0.90358	0.81104	0.82579	1.5529
$^-OOCPZCOO^-$	1	0.45810	0.31482	0.43613	1.3462
HCO_3^-	1	0.99398	0.98015	0.25516	1.3963

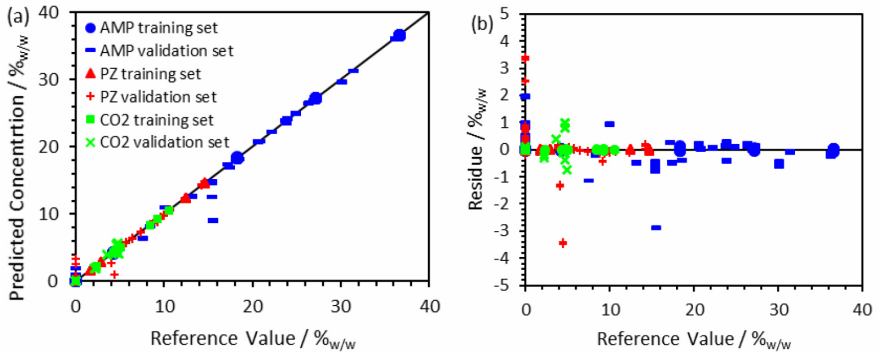

Figure 4. *Prediction and residue of the multiple PLS models*

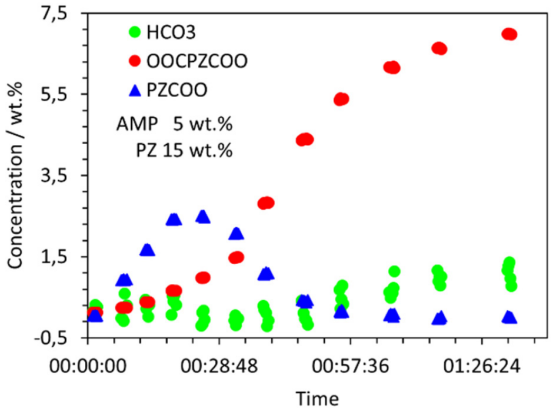

Figure 5. *PZ carbamates and bicarbonate predictions*

with the previous PLS2 model.[9] Although a univariate model would be much simpler and would work as multivariate models to quantify the pure amines. Thanks to the peaks shift and strong overlapping during the carbonation process, the multivariate model had better predictions for the carbamates.

Although both models, PLS and PLS2, had a similar prediction of the concentrations of AMP and PZ, the calibration model uses only the non-carbonated (first point) and the saturated solution (last point). If we compare the middle points, the concentration during the partial carbonation process as shown in Figure 6, the prediction of these amines' concentration was indeed different. We chose these samples as they represent the worst case.

Figure 7 compares the AMP concentration prediction of two PZ solutions. The PLS model performed much better, as no AMP existed on these solutions. The same happened in all PZ solutions, more intensely in the concentrated ones, as shown in Figure 7 (a) and (b). The PZ monocarbamate may be associated with this deviation on the PLS2 model as the AMP prediction happens only at the beginning of the carbonation process. As the partially carbonated solution were all present in the validation set, it can be noted the large increase in the mean error of prediction shown in Tables 3 and 5.

When comparing the PZ prediction in the AMP solutions (Figure 8), the same behavior happens. The points used in the calibration model correctly predicted the zero PZ concentration on both models. When comparing the partial carbonation, the PLS2 failed to predict no PZ.

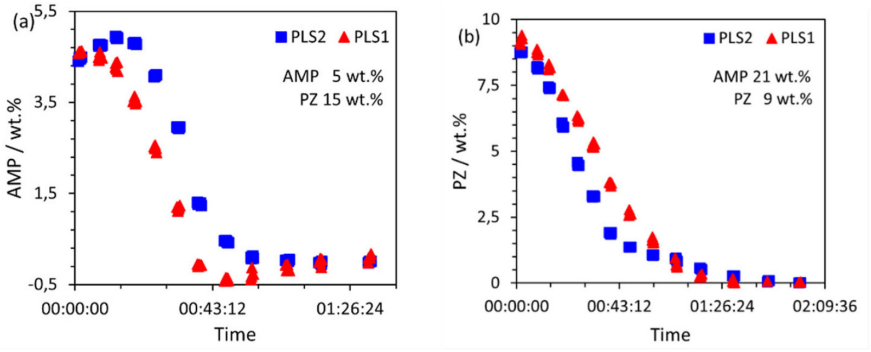

Figure 6. *AMP prediction comparison between PLS and PLS2 models in blend solutions*

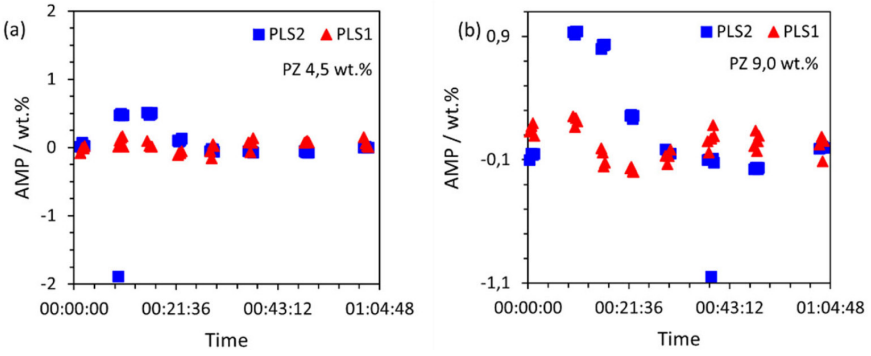

Figure 7. *AMP prediction comparison between PLS and PLS2 models in PZ solutions*

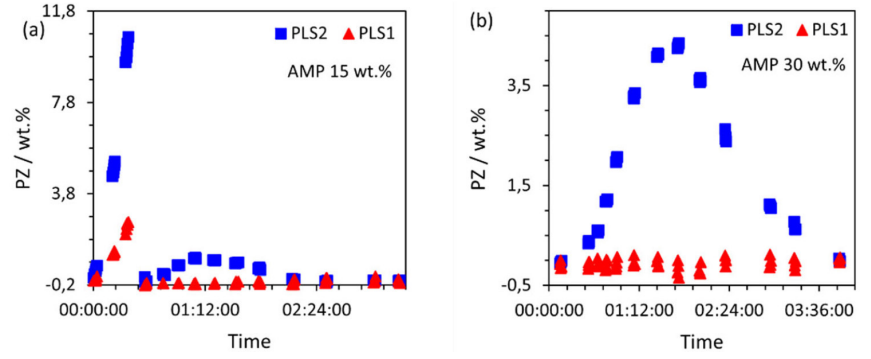

Figure 8. *PZ prediction comparison between PLS and PLS2 models in AMP solutions*

We could infer that the PLS2 model attributed the CO_2 reaction products formed to the quantification of one of the amines due to a broader region used in the model. The PLS model used smaller windows for each species than the PLS2 model. Even gathering all regions together, it was still smaller. So the model had less information and noise, which lead to a better prediction during the carbonation process. Also, we could have overfitted the PLS2 model.

CONCLUSIONS

Using only FTIR spectroscopy allowed the quantification of AMP, PZ, total CO_2, $PZCOO^-$, and HCO_3^- enabling online monitoring of the absorption/desorption process of a CO_2 capture process.

The PLS models showed a significant improvement in predicting the intermediate points of the absorption process compared to the previous PLS2 model.[9] Furthermore, this work used a narrow spectrum region and could extend the quantification of the carbonated reaction products of the amine blend CO_2 reaction.

The differentiation of the CO_2 chemical forms allows a better understanding of the absorption/desorption process in real-time and process optimization since the different CO_2 species need distinctive regeneration temperatures and have varying reaction rates.

SUPPLEMENTARY MATERIAL

The spectra absorbance, concentration, and titration of each sample are available at http://quimicanova.sbq.org.br as an Excel file, with open access.

ACKNOWLEDGMENTS

This work was supported by the CNPq Brazil (Conselho Nacional de Desenvolvimento Científico e Tecnológico) and CAPES (Coordenação de Aperfeiçoamento de Pessoal de Nível Superior).

REFERENCES

1. Rochelle, G. T.; *Science* **2009**, *325*, 1652. [Crossref]
2. Rochelle, G. T.; Chen, E; Freeman, S.; van Wagener, D.; Xu, Q.; Voice, A.; *Chem. Eng. J.* **2011**, *171*, 725. [Crossref]
3. Nwaoha, C.; Saiwan, C.; Tontiwachwuthikul, P.; Supap, T.; Rongwong, W.; Idem, R.; AL-Marri, M. J.; Benamor, A.; *J. Nat. Gas Sci. Eng.* **2016**, *33*, 742. [Crossref]
4. Zhang, W.; Chen, J.; Luo, X.; Wang, M.; *Int. J. Greenhouse Gas Control* **2017**, *63*, 37. [Crossref]
5. Wang, T.; He, H.; Yu, W.; Sharif, Z.; Fang, M.; *Energy Fuels* **2017**, *31*, 4255. [Crossref]
6. Chen, J.; Li, H.; Le, Moullec, Y.; Lu, J.; Marcos, J. C. V.; Chen, G.; *Energy Procedia* **2017**, *114*, 1388. [Crossref]
7. Mores, P.; Scenna, N.; Mussati, S.; *Energy* **2012**, *45*, 1042. [Crossref]
8. Namjoshi, O.; Hatchell, D.; Rochelle, G. T.; *Energy Procedia* **2013**, *37*, 1904. [Crossref]
9. Zanone, A.; Tavares, D. T.; Paiva, J. L. *Vib. Spectrosc.* **2018**, *99*, 156. [Crossref]
10. Krótki, A.; Tatarczuk, A.; Stec, M.; Spietz, T.; Więcław-Solny, L.; Wilk, A.; Cousins, A.; *Greenhouse Gases: Sci. Technol.* **2017**, *7*, 550. [Crossref]
11. Osagie, E.; Biliyok, C.; Di Lorenzo, G.; Manovic, V.; *Energy Procedia* **2017**, *114*, 1930. [Crossref]
12. Hairul, N. A. H.; Shariff, A. M.; Tay, W. H.; Mortel, A. M. A. V. D.; Lau, K. K.; Tan, L. S.; *Sep. Purif. Technol.* **2016**, *165*, 179. [Crossref]
13. Diab, F.; Provost, E.; Laloué, N.; Alix, P.; Souchon, V.; Delpoux, O.; Fürst, W.; *Fluid Phase Equilib.* **2012**, *325*, 90, [Crossref]
14. Kachko, A.; van Der Ham, L. V.; Geers, L. F. G.; Huizinga, A.; Rieder, A.; Abu-Zahra, M. R. M.; Vlugt, T. J. H.; Goetheer, E. L. V.; *Ind. Eng. Chem. Res.* **2015**, *54*, 5769. [Crossref]
15. Kachko, A.; van der Ham, L. V.; Bakker, D. E.; van de Runstraat, A.; Nienoord, M.; Vlugt, T. J. H.; Goetheer, E. L. V.; *Ind. Eng. Chem. Res.* **2016**, *55*, 3804. [Crossref]
16. Mergler, Y.; Rumley-Van Gurp R.; Brasser, P.; De Koning, M.; Goetheer, E.; *Energy Procedia* **2011**, *4*, 259. [Crossref]
17. Geers, L. F. G.; Van De Runstraat, A.; Joh, R.; Schneider, R.; Goetheer, E. L. V.; *Ind. Eng. Chem. Res.* **2011**, *50*, 9175. [Crossref]
18. van Eckeveld, A. C.; van der Ham, L. V.; Geers, L. F. G.; van den Broeke, L. J. P.; Boersma, B. J.; Goetheer, E. L. V.; *Ind. Eng. Chem. Res.* **2014**, *53*, 5515. [Crossref]
19. van Der Ham, L. V.; van Eckeveld, A. C.; Goetheer, E. L. V.; *Energy Procedia* **2014**, *63*, 1223. [Crossref]
20. Kachko, A.; van der Ham, L. V.; Bardow, A.; Vlugt, T. J. H.; Goetheer, E. L. V.; *Int. J. Greenhouse Gas Control* **2016**, *47*, 17. [Crossref]
21. du Preez, L. J.; Callanan, L. H.; Knoetze, J. H.; *Vib. Spectrosc.* **2018**, *99*, 25. [Crossref]
22. Jackson, P.; Robinson, K.; Puxty, G.; Attalla, M. I.; *Energy Procedia* **2009**, *1*, 985. [Crossref]]
23. Richner, G.; Puxty, G.; *Ind. Eng. Chem. Res.* **2012**, 51, 14317. [Crossref]
24. Robinson, K.; McCluskey, A.; Attalla, M. I.; *ChemPhysChem* **2012**, *13*, 2331. [Crossref]
25. Ermatchkov, V.; Pérez-Salado, K. A.; Maurer, G.; *J. Chem. Thermodyn.* **2003**, *35*, 1277. [Crossref]
26. Li, H.; Frailie, P. T.; Rochelle, G. T.; Chen, J.; *Chem. Eng. Sci.* **2014**, *117*, 331. [Crossref]
27. Agbonghae, E. O.; Hughes, K. J.; Ingham, D. B.; Ma, L.; Pourkashanian, M.; *Ind. Eng. Chem. Res.* **2014**, *53*, 14815. [Crossref]
28. Sartori, G.; Savage, D. W.; *Ind. Eng. Chem. Fundam.* **1983**, *22,* 239. [Crossref]
29. Tavares, D. T.; *Dissertação de Mestrado*, Universidade de São Paulo, Brasil, 2015. [Crossref]
30. Rodriguez-Flores, H. A.; Salvagnini, W. M.; Trigilio, D. T.; Paiva, J. L.; *International Conference in Greenhouse Gas Technologies*, Austin, 2014.
31. Xu, S.; Wang, Y. W.; Otto, F. D.; Mather, A. E.; *Chem. Eng. Sci.* **1996**, *51*, 841. [Crossref]
32. Du, Y. P.; Liang, Y. Z.; Jiang, J. H.; Berry, R. J.; Ozaki, Y.; *Anal. Chim. Acta.* **2004**, *501*, 183. [Crossref]
33. Rudolph, W. W.; Fischer, D.; Irmer, G.; *Appl. Spectrosc.* **2006**, *60*, 130. [Crossref]
34. Garand, E.; Wende, T.; Goebbert, D. J.; Bergmann, R.; Meijer, G.; Neumark, D. M.; Asmis, K.; *J. Am. Chem. Soc.* **2010**, *132*, 849. [Crossref]